学位論文　博士（医学）甲

Lysosomal targeting of SIDT2 via multiple YxxΦ motifs is required for SIDT2 function in the process of RNautophagy
（複数のYxxΦモチーフを介したSIDT2のリソソーム局在はRNautophagyにおけるSIDT2の機能に必要である）

Contu Viorica Raluca

山梨大学

© 2017. Published by The Company of Biologists Ltd | Journal of Cell Science (2017) 130, 2843-2853 doi:10.1242/jcs.202481

RESEARCH ARTICLE

Lysosomal targeting of SIDT2 via multiple YxxΦ motifs is required for SIDT2 function in the process of RNautophagy

Viorica Raluca Contu[1,2], Katsunori Hase[1,3], Hiroko Kozuka-Hata[4], Masaaki Oyama[4], Yuuki Fujiwara[1], Chihana Kabuta[1], Masayuki Takahashi[1], Fumihiko Hakuno[3], Shin-Ichiro Takahashi[3], Keiji Wada[1] and Tomohiro Kabuta[1,*]

ABSTRACT

RNA degradation is an essential process for maintaining cellular homeostasis. Previously, we discovered a novel RNA degradation system, RNautophagy, during which direct import of RNA into lysosomes in an ATP-dependent manner followed by degradation takes place. The putative nucleic acid transporter SID-1 transmembrane family member 2 (SIDT2) predominantly localizes to lysosomes and mediates the translocation of RNA into lysosomes during RNautophagy. However, little is known about the mechanisms of sorting SIDT2 to lysosomes. Here, we show that three cytosolic YxxΦ motifs (in which x is any amino acid and Φ is an amino acid with a bulky hydrophobic side chain) are required for the lysosomal localization of SIDT2, and that SIDT2 interacts with adaptor protein complexes AP-1 and AP-2. We also find that localization to lysosomes by these three motifs is necessary for SIDT2 function in the process of RNautophagy, and that SIDT2 strikingly increases endogenous RNA degradation at the cellular level. To our knowledge, this is the first study to report an endogenous intracellular protein for which overexpression substantially increased intracellular RNA degradation. This study provides new insight into lysosomal targeting of proteins and intracellular RNA degradation, and further confirms the critical function of SIDT2 in RNautophagy.

This article has an associated First Person interview with the first author of the paper.

KEY WORDS: RNautophagy, SIDT2, YxxΦ motif, RNA degradation, Lysosome

INTRODUCTION

Both protein-coding and noncoding RNAs are continuously synthesized and degraded in cells to ensure the proper function of cellular processes. Processing, quality control and turnover of RNA are crucial for correct gene expression, and removal of unnecessary or aberrant RNA through degradation pathways constantly occurs to maintain RNA homeostasis (Jackowiak et al., 2011). Nuclear or cytoplasmic RNA degradation has been extensively investigated; three categories of ribonucleases (endonucleases, 3′ exonucleases and 5′ exonucleases) break down RNA, assisted by various helicases, polymerases and chaperones (Houseley and Tollervey, 2009). However, little research has been conducted on RNA degradation by lysosomes, the major organelles in charge of macromolecule breakdown (Frankel et al., 2017; Fujiwara et al., 2017). RNase T2 is the main lysosomal ribonuclease; defects in *RNASET2* have been reported to cause cystic leukoencephalopathy in humans, and suggested to interfere with brain development through RNA metabolism (Haud et al., 2011; Henneke et al., 2009). RNA degradation by lysosomes may be considerably involved in human diseases, and therefore requires further investigation.

We have recently discovered RNautophagy/DNautophagy (RDA), a novel RNA/DNA degradation process performed by lysosomes, in which RNA/DNA is directly imported into lysosomes in an ATP-dependent manner and then degraded (Fujiwara et al., 2013a,b). We have also found that, to some extent, RDA exhibits substrate selectivity *in vitro* at the step of uptake into lysosomes (Hase et al., 2015), and that the lysosomal membrane protein LAMP2C can bind to RNA/DNA through its carboxyl-terminal cytosolic tail and function as an RNA/DNA receptor (Fujiwara et al., 2013a, 2015). One of our latest studies has revealed that SID-1 transmembrane family member 2 (SIDT2) mediates the translocation of RNA/DNA across the lysosomal membrane during RDA, and that SIDT2-mediated RNautophagy is an important pathway for intracellular RNA degradation, at least in mouse embryonic fibroblasts (MEFs) (Aizawa et al., 2017, 2016). SIDT2 is one of the two mammalian orthologs (SIDT1 and SIDT2) of the *Caenorhabditis elegans* putative RNA transporter, systemic RNA interference defective protein 1 (SID-1), but unlike SID-1 and SIDT1, which have been reported to mainly localize to the plasma membrane (Duxbury et al., 2005; Feinberg and Hunter, 2003), SIDT2 has been observed to predominantly localize to lysosomes (Aizawa et al., 2016; Chapel et al., 2013; Jialin et al., 2010; Schröder et al., 2007). Inconsistent with the lysosomal membrane proteins that have been investigated so far, SIDT2 contains no potential sorting motif in its carboxyl terminus cytoplasmic tail. Although two potential tyrosine-type sorting motifs, located in the cytosolic region of SIDT2 between transmembrane domains 1 and 2, have been inferred from a bioinformatics analysis, the molecular signals responsible for the lysosomal targeting of SIDT2 have remained elusive (Jialin et al., 2010). SIDT2 appears to play a significant role in lysosomal degradation of RNA; therefore, characterization of its molecular signals is necessary for deeper understanding of RNA degradation and cellular homeostasis.

In this study, we found that SIDT2 strikingly increases intracellular degradation of endogenous RNA. We also showed that SIDT2 interacts with adaptor protein (AP) complexes AP-1 and AP-2, and that the targeting of SIDT2 to the lysosomal membrane is mediated by three tyrosine-based YxxΦ motifs (Y^{359}GSF, Y^{410}DTL and Y^{428}LCV). We conclude that localization to lysosomes by these motifs is required for SIDT2 function during RNautophagy.

[1]Department of Degenerative Neurological Diseases, National Institute of Neuroscience, National Center of Neurology and Psychiatry, Kodaira, Tokyo 187-8502, Japan. [2]Department of Neurology, Interdisciplinary Graduate School of Medicine and Engineering, University of Yamanashi, Chuo, Yamanashi 409-3898, Japan. [3]Department of Animal Sciences and Applied Biological Chemistry, Graduate School of Agriculture and Life Sciences, The University of Tokyo, 1-1-1 Yayoi, Bunkyo-ku, Tokyo 113-8657, Japan. [4]Medical Proteomics Laboratory, The Institute of Medical Science, The University of Tokyo, 4-6-1 Shirokanedai, Minato-ku, Tokyo 108-8639, Japan.

*Author for correspondence (kabuta@ncnp.go.jp)

Received 10 February 2017; Accepted 10 July 2017

Journal of Cell Science (2017) 130, 2843-2853 doi:10.1242/jcs.202481

RESULTS

SIDT2 overexpression drastically increases intracellular degradation of endogenous RNA

We have recently reported that SIDT2 mediates the uptake of RNA in the process of RNautophagy, and that knockdown of *Sidt2* strongly inhibited the degradation of endogenous RNA by lysosomes at the cellular level in MEFs (Aizawa et al., 2016). Therefore, we next investigated the effect of SIDT2 overexpression on the intracellular degradation of endogenous RNA. To this end, we labeled endogenous RNA of control cells and of cells overexpressing SIDT2 with [^{3}H]uridine, and then measured the radioactivity of the labeled RNA at 0 and 24 h (Fig. 1A). Strikingly, overexpression of SIDT2 led to a ∼1.7-fold increase in the levels of degraded RNA in Neuro2a cells (Fig. 1B,C).

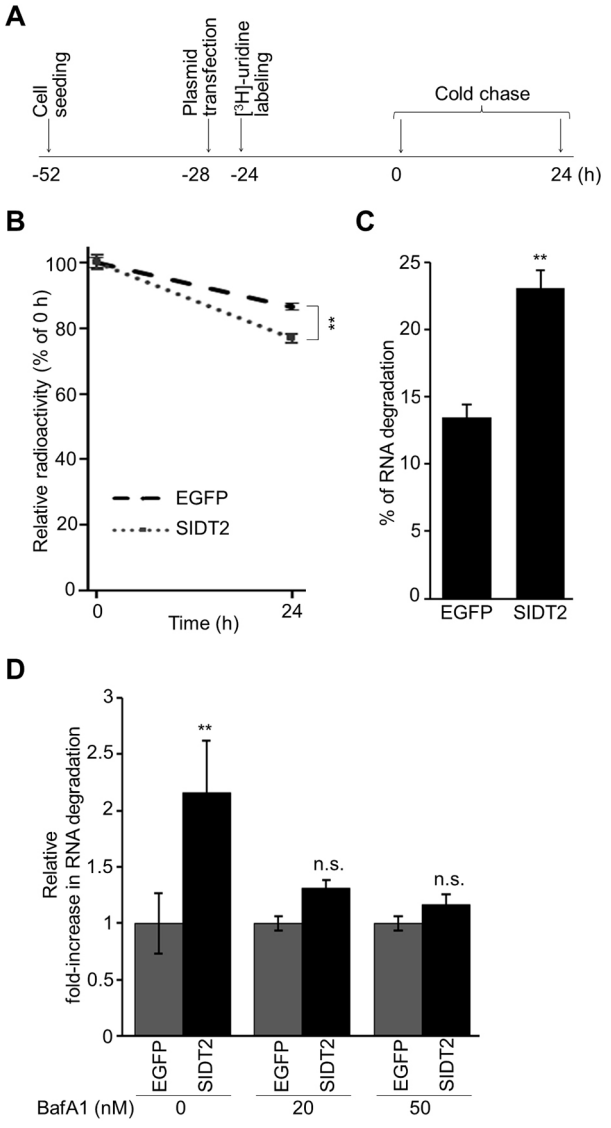

Fig. 1. SIDT2 overexpression drastically increases intracellular degradation of endogenous RNA. (A) Scheme of the experimental method for measuring intracellular degradation of endogenous RNA. (B–D) Neuro2a cells were transfected with EGFP- or SIDT2-expressing vectors, then cells were exposed to 0.012 pM [^{3}H]uridine for 24 h to label intracellular RNA. Next, cells were rinsed and grown in culture medium containing (B,C) 5 mM unlabeled uridine and (D) 20 or 50 nM BafA1. After 0 and 24 h, cells were harvested and acid-insoluble radioactivity was measured and expressed as a (B) percentage of that at 0 h, (C) percentage of degraded RNA, or (D) fold-increase in RNA degradation relative to EGFP. Data are mean±s.d. (n=4). **P<0.01 vs EGFP; n.s., not significant vs EGFP (Tukey-Kramer test).

To show that this increase is caused by lysosomal degradation of RNA, we treated the cells during cold chase with Bafilomycin A1 (BafA1), a specific inhibitor of the lysosomal vacuolar-type H^+-ATPase, and then investigated the effect of SIDT2 overexpression on intracellular RNA degradation. Overexpression of SIDT2 failed to significantly increase the levels of degraded RNA in BafA1-treated Neuro2a cells (Fig. 1D), indicating that the enhanced RNA degradation observed in SIDT2-overexpressing cells occurs at the lysosomes. Taken together with the findings of our previous study (Aizawa et al., 2016), these results strongly suggest that SIDT2 plays a key role in the degradation of endogenous RNA at the cellular level.

SIDT2 localization to lysosomes requires multiple YxxΦ motifs

Next, we investigated the mechanisms of SIDT2 targeting the lysosomal membrane. An analysis of the amino acid sequence of murine SIDT2 revealed three possible YxxΦ-type sorting motifs (in which x is any amino acid and Φ is an amino acid with a bulky hydrophobic side chain), conserved among various species (Fig. 2A), in the cytosolic region between transmembrane domains 1 and 2 (Y^{359}GSF, Y^{410}DTL and Y^{428}LCV); we also observed a Yxx sequence of amino acids (Y^{830}VF) at the carboxyl terminus of SIDT2 (Fig. 2B,C). Because most lysosomal membrane proteins have been reported to have their sorting motifs situated at the carboxyl terminus (Bonifacino and Traub, 2003), we also investigated the possible involvement of the Yxx sequence in the lysosomal localization of SIDT2 together with the three motifs. We generated plasmids that express serine instead of each of the tyrosines (Y359, Y410, Y428 and Y830) in EGFP-fused wild-type (WT) SIDT2 (SIDT2-EGFP). These plasmids were transfected into Neuro2a cells, and the intracellular localization of $SIDT2^{WT}$ and of the mutants was examined. Because the YxxΦ motifs do not tolerate substitutions in place of tyrosine, any tyrosine mutation disrupts the function of the YxxΦ motif (Bonifacino and Traub, 2003). $SIDT2^{Y830S}$ was localized as efficiently as $SIDT2^{WT}$ to lysosomes (Fig. 2D,H), whereas interruption of any of the three YxxΦ motifs visibly altered the lysosomal localization of SIDT2 (Fig. 2E–G). The Y359S, Y410S and Y428S mutations significantly reduced the colocalization rate of SIDT2 with LysoTracker Red (LT) to 55.9%, 21.4% and 14.3%, respectively (Fig. 2I). However, the single motif disruptions did not completely abolish SIDT2 localization to lysosomes.

We next mutagenized the three YxxΦ motifs in all possible combinations (Fig. 3A) and examined the localization of the mutants (Fig. 3B–E). Disruption of any two YxxΦ motifs was significantly more efficient in decreasing the colocalization rate of SIDT2 with LT than disruption of just Y^{410}DTL or Y^{428}LCV, the motifs that decreased the colocalization rate of SIDT2 with LT the most (Fig. 3G), and disruption of the three motifs almost completely abolished localization of SIDT2 to the lysosomal membrane (Fig. 3E, H). Addition of the Y830S mutation to $SIDT2^{3YS}$ did not change the colocalization rate of $SIDT2^{3YS}$ (Fig. 3E,F,H). Collectively, these data indicate that the three YxxΦ motifs (Y^{359}GSF, Y^{410}DTL and Y^{428}LCV), but not the Y^{830}VF sequence, are required for the lysosomal localization of SIDT2.

SIDT2 interacts with AP-1 and AP-2

Intracellular trafficking of membrane proteins is generally facilitated by AP complexes (Bonifacino and Traub, 2003; Braulke and Bonifacino, 2009; Park and Guo, 2014). We next performed an

Journal of Cell Science (2017) 130, 2843-2853 doi:10.1242/jcs.202481

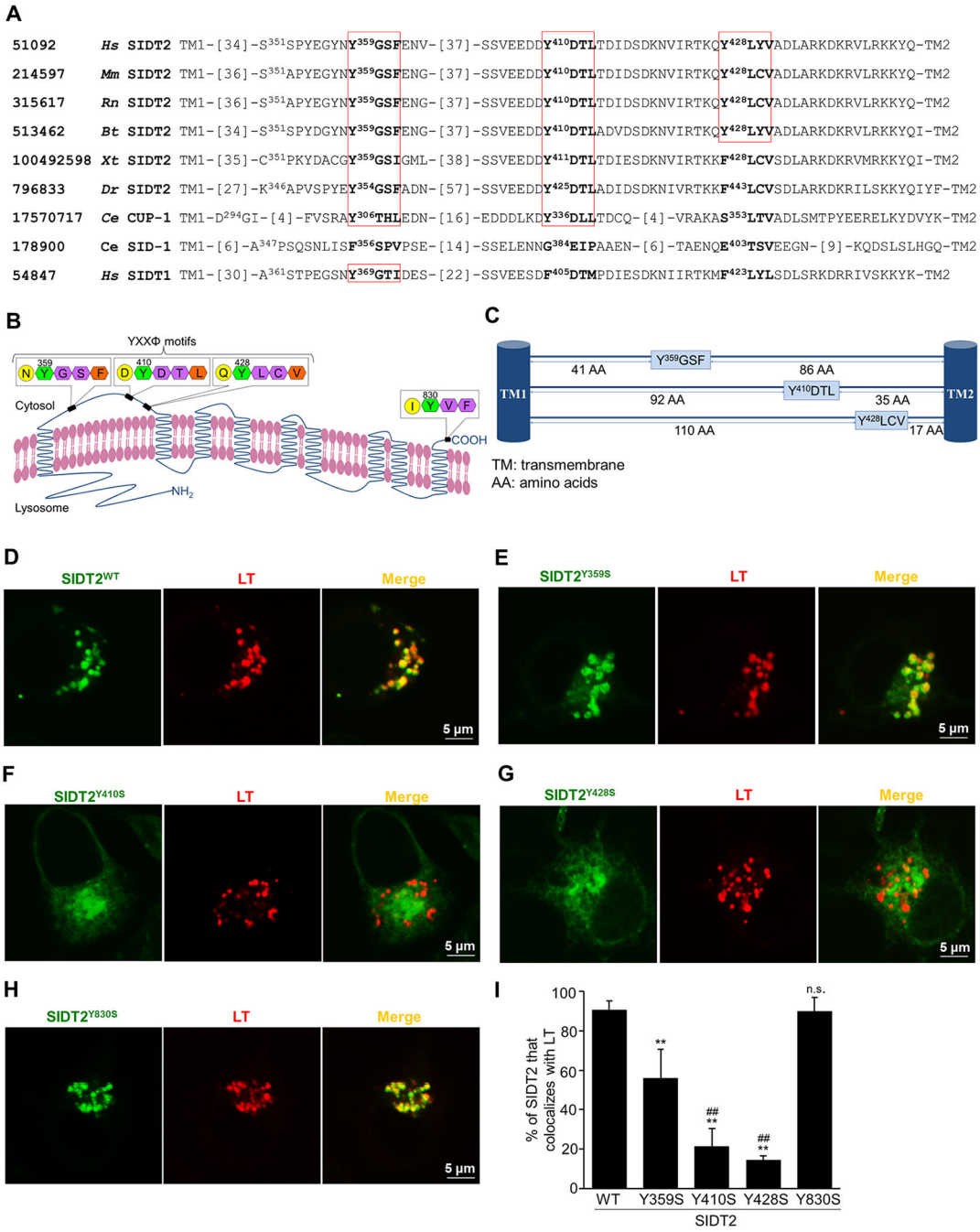

Fig. 2. A single YxxΦ motif disruption impairs localization of SIDT2 to lysosomes. (A) Sequences of the cytosolic regions between transmembrane 1 and 2 of several proteins. On the left are the NCBI gene identification numbers of the proteins, followed by the species names and the common names of the proteins. *Hs*, *Homo sapiens*; *Mm*, *Mus musculus*; *Rn*, *Rattus norvegicus*; *Bt*, *Bos taurus*; *Xt*, *X. tropicalis*; *Dr*, *D. rerio*; *Ce*, *C. elegans*. YxxΦ motifs are boxed in red. The number of omitted residues is shown between square brackets. The superscripts placed at the right of some residues show the residues' numbers. The amino acid sequences between transmembrane 1 and 2 are shown based on the protein information provided by the UniProt database. (B) The topology of murine SIDT2 and the position of possible YxxΦ motifs within the cytosolic domains. A free Motifolio vector graphic was used for the lipid bilayer drawing (www.motifolio.com). The diagram was drawn based on the information about murine SIDT2 provided by the UniProt database (http://www.uniprot.org/uniprot/Q8CIF6). (C) Diagram representing the position of the YxxΦ motifs within the first cytosolic domain of SIDT2 and the distance to the cytoplasmic transmembrane domains. The diagram was designed based on the information about murine SIDT2 provided by the UniProt database. (D) WT SIDT2-EGFP or (E–H) SIDT2-EGFP with a single tyrosine substitution was expressed in Neuro2a cells, and then lysosomes were stained with LT. Image acquisition was performed using a confocal laser-scanning microscope. (I) The colocalization rates in D–H were quantified using ImageJ. Data are mean±s.d. (n=4–6). $^{**}P$<0.01 vs WT; n.s., not significant vs WT; $^{\#\#}P$<0.01 vs Y359S (Tukey-Kramer test). Scale bars: 5 μm.

immunoprecipitation (IP) assay to investigate whether SIDT2 interacts with the AP complexes. After overexpression in Neuro2a cells, IP of FLAG-tagged SIDT2 was conducted from the cell lysates and the IP product was subjected to shotgun proteomic analysis. Several subunits of the AP-1 (β1, μ1) and AP-2 (α1, α2, β, μ), but none of the AP-3 or AP-4 complexes, were detected as SIDT2-interacting proteins (Table 1; Table S1). To further confirm these results, we also immunoblotted the IP product and found that

Journal of Cell Science (2017) 130, 2843-2853 doi:10.1242/jcs.202481

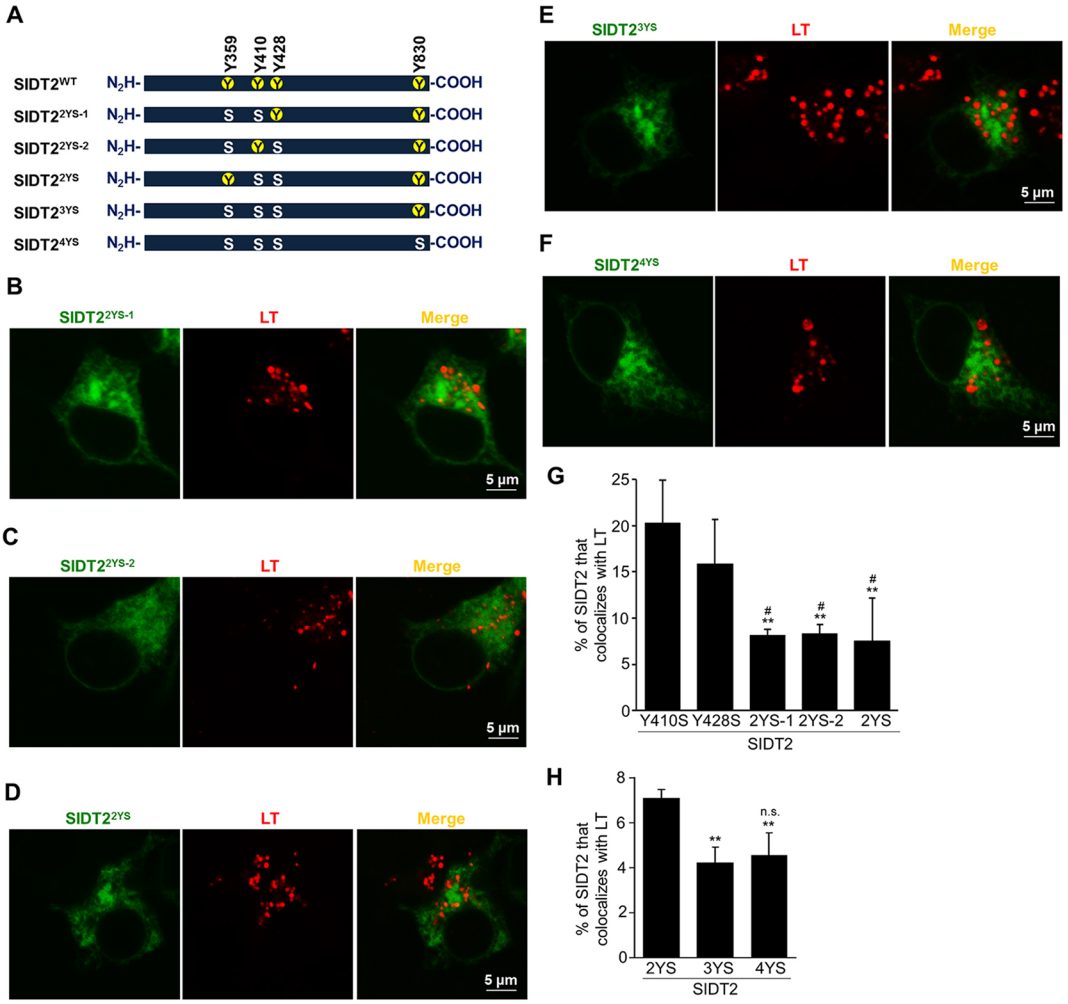

Fig. 3. SIDT2 localization to lysosomes requires three YxxΦ motifs. (A) Abbreviations of multiple tyrosine to serine substitutions. (B–F) SIDT2-EGFP with multiple tyrosine substitutions was expressed in Neuro2a cells, and then lysosomes were stained with LT. Image acquisition was performed using a confocal laser-scanning microscope. (G,H) The colocalization rates in B–F were quantified using ImageJ. Data are mean±s.d. (n=5). (G) $^{**}P$<0.01 vs Y410S; $^{\#}P$<0.05 vs Y428S (Tukey-Kramer test). (H) $^{**}P$<0.01 vs 2YS; n.s., not significant vs 3YS (Tukey-Kramer test). Scale bars: 5 µm.

γ-adaptin, a component of the AP-1 complex, and α-adaptin, a component of the AP-2 complex, coimmunoprecipitated with SIDT2, but no interaction between SIDT2 and AP-3 µ1 subunit or AP-4 µ1 subunit was detected (Fig. 4A).

Complexes AP-1 and AP-2 interact with tyrosine-based sorting motifs (Park and Guo, 2014). To clarify whether SIDT2 interacts with AP-1 and AP-2 complexes through the YxxΦ motifs, we performed coimmunoprecipitation (coIP) analysis of two and three YxxΦ motif-disrupted mutants of FLAG-tagged SIDT2. $SIDT2^{2YS}$ and $SIDT2^{WT}$ pulled down γ-adaptin and α-adaptin at comparable levels, while $SIDT2^{3YS}$, $SIDT2^{2YS-1}$ and $SIDT2^{2YS-2}$ pulled down less γ-adaptin/α-adaptin than $SIDT2^{WT}$ (Fig. 4B). These results suggest that SIDT2 interacts with AP-1 and AP-2 complexes mainly through the Y^{359}GSF motif.

Table 1. AP subunits identified by shotgun proteomic analysis

Protein name	Score	Matching peptides	Sequence coverage (%)
AP-2 complex subunit β isoform b	473.5	12	20.6
AP-1 complex subunit β1 isoform 2	294.0	8	10.71
AP-2 complex subunit α1 isoform b	250	6	9.74
AP-2 complex subunit α2	201.3	4	7.57
AP-1 complex subunit µ1	121.6	3	11.82
AP-2 complex subunit µ	90.1	4	11.26

Untagged $SIDT2^{WT}$ (control) or FLAG-tagged $SIDT2^{WT}$ were expressed in Neuro2a cells, then the cell lysates were subjected to IP using an anti-FLAG antibody, and shotgun proteomic analysis of the IP products was performed. Peptides corresponding to AP-1 or AP-2 subunits were not detected in the IP product from the control sample.

SIDT2-mediated RNautophagy requires localization of SIDT2 to lysosomes via three YxxΦ motifs *in vitro*

SIDT2 mediates RNA uptake by lysosomes during RNautophagy (Aizawa et al., 2016). We next determined whether targeting of SIDT2 to the lysosomal membrane is required for SIDT2 function. Neuro2a cells were transfected with expression vectors that produce untagged full-length $SIDT2^{WT}$, $SIDT2^{2YS}$ or $SIDT2^{3YS}$. Overexpression was then confirmed by western blot analysis (Fig. 5A; Fig. S1). Next, lysosomes were isolated and an RNA uptake assay was performed (Fujiwara et al., 2013a). Isolated lysosomes were incubated with RNA in the presence of ATP, and then lysosomes were removed by centrifugation and the RNA levels in the solution outside the lysosomes were quantified. Overexpression of $SIDT2^{WT}$ or $SIDT2^{2YS}$ significantly increased

Journal of Cell Science (2017) 130, 2843-2853 doi:10.1242/jcs.202481

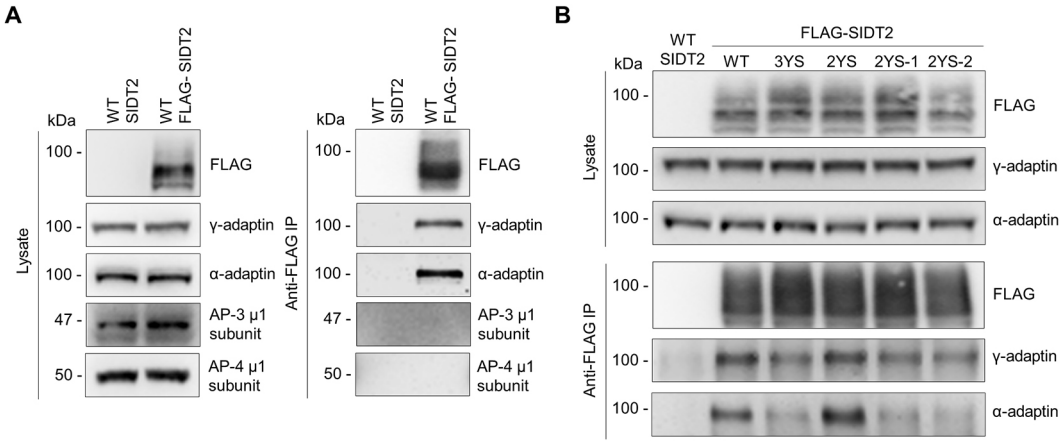

Fig. 4. SIDT2 interacts with AP-1 and AP-2. (A,B) SIDT2^{WT}, FLAG-tagged SIDT2^{WT} or FLAG-tagged SIDT2 with multiple tyrosine substitutions were expressed in Neuro2a cells, then the cells were harvested and suspended in a lysis buffer supplemented with protease and phosphatase inhibitors. After incubation at 4°C with rotation, cell lysates were centrifuged and the supernatant was subjected to IP using an anti-FLAG antibody, and the resulting samples and cell lysates immunoblotted for the indicated proteins.

the RNA uptake activity of lysosomes compared with the control lysosomes, whereas overexpression of SIDT2^{3YS} led to no change in RNautophagy activity (Fig. 5B). We also performed RNA uptake assays using lysosomes that were derived from SIDT2^{WT}- or SIDT2^{Y830S}-overexpressing cells (Fig. 5C), and found that the Y830S mutation did not alter SIDT2 function during RNautophagy

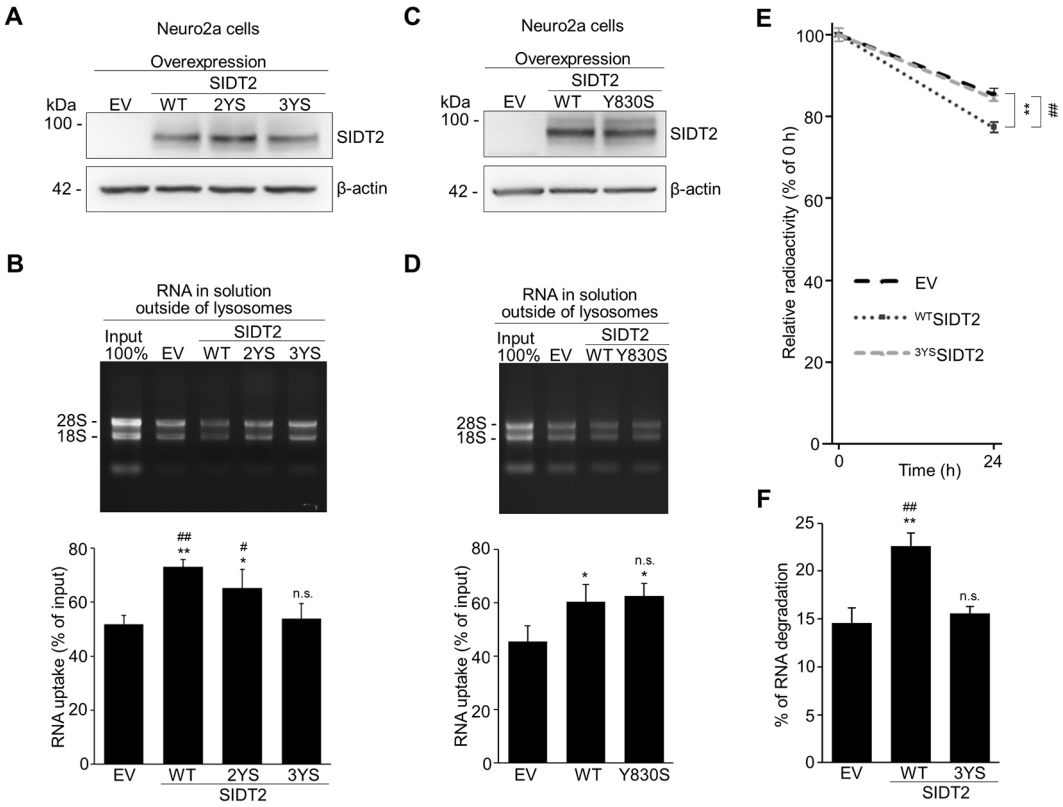

Fig. 5. Localization to lysosomes via three YxxΦ motifs is required for SIDT2 function *in vitro* and at the cellular level. (A,C) Neuro2a cells were transfected with empty vector (EV), WT or tyrosine mutants of SIDT2-expressing vectors. After 48 h, cells were harvested and the levels of SIDT2 and β-actin were measured by western blot analysis. (B,D) Neuro2a cells were transfected with EV, WT or tyrosine mutants of SIDT2-expressing vectors. After 48 h, lysosomes were isolated by density gradient ultracentrifugation and RNA uptake assays were performed. Lysosomes (20–30 μg protein) were incubated with 5 μg total RNA (purified from mouse brains) for 3 min at 37°C in the presence of ATP, and then lysosomes were precipitated by centrifugation, and RNA levels in the solution outside the lysosomes were measured. RNA uptake levels were calculated by subtracting the RNA levels in the solution outside the lysosomes from the RNA input levels. Data are mean±s.d. (B) **P*<0.05, ***P*<0.01 vs EV; n.s., not significant vs EV; $^{\#}$*P*<0.05, $^{\#\#}$*P*<0.01 vs 3YS; *n*=4 (Tukey-Kramer test). (D) **P*<0.05 vs EV; n.s., not significant vs EV (Tukey-Kramer test); *n*=3. (E,F) WT or the 3YS mutant of SIDT2 was overexpressed in Neuro2a cells, which were then exposed to 0.012 pM [^{3}H]uridine for 24 h to label intracellular RNA. Next, the cells were rinsed and grown in culture medium containing 5 mM unlabeled uridine. After 0 and 24 h the cells were harvested, and then acid-insoluble radioactivity was measured and expressed as a percentage of (A) 0 h or (B) degraded RNA. Data are mean±s.d. (*n*=4). ***P*<0.01 vs EV; $^{\#\#}$*P*<0.01 vs 3YS; n.s., not significant vs EV (Tukey-Kramer test).

Journal of Cell Science (2017) 130, 2843-2853 doi:10.1242/jcs.202481

(Fig. 5D). These data confirmed our previous findings that SIDT2 mediates RNA uptake by lysosomes, and showed that localization to lysosomes via the Y^{359}GSF, Y^{410}DTL and Y^{428}LCV motifs is required for SIDT2 function during RNautophagy *in vitro*.

SIDT2^{3YS} does not increase the intracellular degradation of endogenous RNA

To elucidate whether targeting of SIDT2 to the lysosomal membrane is required for the function of SIDT2 at the cellular level, we labeled endogenous RNA of control cells, and cells overexpressing SIDT2^{WT} or SIDT2^{3YS} with [^{3}H]uridine, and then measured the radioactivity of the labeled RNA at 0 and 24 h postlabeling (Fig. 1A). A ∼1.6-fold increase in the level of degraded RNA was observed when SIDT2^{WT} was overexpressed in Neuro2a cells compared with the control cells, whereas no significant increase occurred in the case of SIDT2^{3YS} overexpression (Fig. 5E,F). These results suggest that Y^{359}GSF, Y^{410}DTL and Y^{428}LCV motifs are required for SIDT2-mediated intracellular degradation of endogenous RNA.

To further support the idea that delocalization of SIDT2^{3YS} itself from the lysosomal membrane results in stagnation of the lysosomal RNA degradation mediated by SIDT2 overexpression, we inserted YxxΦ motifs into SIDT2^{3YS} and investigated whether SIDT2^{3YS} is redirected to the lysosomes and recovers its function. The YxxΦ motifs of the well-characterized murine lysosomal membrane proteins LAMP2A (YEQF), LAMP2B (YQTL) and LAMP2C (YQSF) were inserted in different combinations just before S359, S410 and S428 of SIDT2^{3YS}, respectively (Fig. 6A), and we then observed the localization of the resulting mutants. Insertion of YEQF and YQSF into EGFP-fused SIDT2^{3YS} (SIDT2^{3YS+A}, SIDT2^{3YS+AC}, SIDT23YS^{+ABC}) redirected SIDT2^{3YS} to the lysosomal membrane (Fig. 6B–E). Next, we investigated the effect of the redirected mutants on intracellular RNA degradation. Overexpression of SIDT2^{3YS+AC} or SIDT2$^{3YS+ABC}$ significantly increased the level of degraded RNA at the cellular level in comparison to SIDT2^{3YS} (Fig. 6F). Together, these data indicate that lysosomal localization of SIDT2 is required for SIDT2-mediated intracellular degradation of endogenous RNA, and that the increase in degradation of endogenous RNA at the cellular level observed in SIDT2-overexpressing cells was due to RNA degradation by the lysosomes.

YGSF, YDTL and YLCV are indeed functional YxxΦ motifs

We have previously reported that SIDT1, the other mammalian ortholog of the putative RNA transporter SID-1, scarcely localizes to the lysosomal membrane and does not increase RNautophagy *in vitro* following overexpression (Aizawa et al., 2016). To further confirm that Y^{359}GSF, Y^{410}DTL and Y^{428}LCV motifs of SIDT2 are functional, we first inserted mutations in SIDT1, so that it contained the three motifs in the predicted conserved positions (Fig. 2A and Fig. 6G). Then, we investigated the localization and ability to increase intracellular RNA degradation of the resulting mutant (SIDT1^{3YxxΦ}) and of SIDT1^{WT}. SIDT1^{WT} scarcely colocalized with LT (Fig. 6H), consistent with our previous report (Aizawa et al., 2016). By contrast, SIDT1^{3YxxΦ} was found to mainly localize to the lysosomes (Fig. 6I). Overexpression of SIDT1^{WT} tended to enhance intracellular RNA degradation, while overexpression of SIDT1^{3YxxΦ} increased the levels of degraded RNA as readily as SIDT2 (Fig. 6J). Taken together, these results indicate that YGSF, YDTL and YLCV are indeed functional YxxΦ motifs.

SIDT2^{3YS} accumulates in the Golgi complex

SIDT2^{3YS} mainly localized to intracellular compartments in proximity of the nucleus (Fig. 3E). We considered that SIDT2^{3YS} may accumulate in the endoplasmic reticulum (ER). After overexpressing WT or the 3YS mutant of SIDT2-EGFP in Neuro2a cells, the ER was stained using an ER-ID Red assay kit, and colocalization of SIDT2 and the ER was examined. Both SIDT2^{3YS} and SIDT2^{WT} did not overlap with the ER (Fig. 7A,B). These results suggest that disruption of the Y^{359}GSF, Y^{410}DTL and Y^{428}LCV motifs does not impair the trafficking of SIDT2 from the ER to the Golgi complex.

We next investigated whether SIDT2^{3YS} accumulates in the Golgi complex. We used Golgi-RFP to stain the Golgi complex in Neuro2a cells overexpressing WT or the 3YS mutant of SIDT2-EGFP, and examined the localization of SIDT2. Accumulation of SIDT2^{3YS} in the Golgi complex was clearly observed, while SIDT2^{WT} almost did not colocalize with the Golgi marker (Fig. 7C,D). Similar results were obtained when GM130 protein was immunostained as the Golgi marker (Fig. 7E,F). Taken together, these results showed that SIDT2 that lacks the signals targeting it to the lysosomal membrane accumulated in the Golgi complex.

DISCUSSION

Our current study has revealed that SIDT2 localization to the lysosomal membrane is mediated by three cytosolic YxxΦ motifs located between transmembrane 1 and 2, and that SIDT2 interacts with AP-1 and AP-2 mainly through the Y^{359}GSF motif. In addition, SIDT2 targeting to lysosomes via the three motifs is necessary for SIDT2 function in the process of RNautophagy *in vitro* and at the cellular level.

We showed that overexpression of SIDT2 markedly increased degradation of endogenous RNA at the cellular level (Fig. 1B,C). Extensive research on RNA degradation has been conducted and many proteins that take part in the process have been identified (Houseley and Tollervey, 2009). However, to the best of our knowledge, this is the first study to report an endogenous intracellular protein for which overexpression substantially increased intracellular RNA degradation. We also found that BafA1 treatment hindered the SIDT2-mediated increase in intracellular RNA degradation (Fig. 1D), and that localization to the lysosomal membrane is necessary for SIDT2 function in the process of RNautophagy both *in vitro* and at the cellular level (Fig. 5). These results indicated that the increase in endogenous RNA degradation at the cellular level following SIDT2 overexpression was caused by RNA degradation by lysosomes. We have previously reported that knockdown of *Sidt2* inhibited up to 50% of total RNA degradation in MEFs, and that the inhibition was mainly due to inhibition of lysosomal function (Aizawa et al., 2016). Taken together, these data strongly suggest that SIDT2 plays a key role in maintaining intracellular RNA homeostasis.

We showed that lysosomal localization of SIDT2 was mediated by three YxxΦ motifs (Y^{359}GSF, Y^{410}DTL and Y^{428}LCV), which are situated in the cytosolic region of SIDT2, between transmembrane domains 1 and 2 (Fig. 2A–C). The YxxΦ motifs that encode lysosomal targeting signals are generally situated 6–13 residues from the transmembrane domain at the carboxyl terminus of the protein and, as far as we know, all lysosomal proteins identified so far contain one functional YxxΦ motif (Bonifacino and Traub, 2003; Braulke and Bonifacino, 2009). The amino acids that constitute or precede the YxxΦ motifs also influence the lysosomal targeting. Acidic amino acids at the X positions, or glycine preceding the motifs, seem to favor lysosomal targeting. This is the case with LAMP2A, for example, which is one of the best-characterized lysosomal proteins thus far (Braulke and Bonifacino, 2009). Interestingly, the Y^{359}GSF, Y^{410}DTL and Y^{428}LCV motifs, which mediate the lysosomal localization of SIDT2, are situated 41, 35 and 17 residues from the transmembrane domain, respectively

Journal of Cell Science (2017) 130, 2843-2853 doi:10.1242/jcs.202481

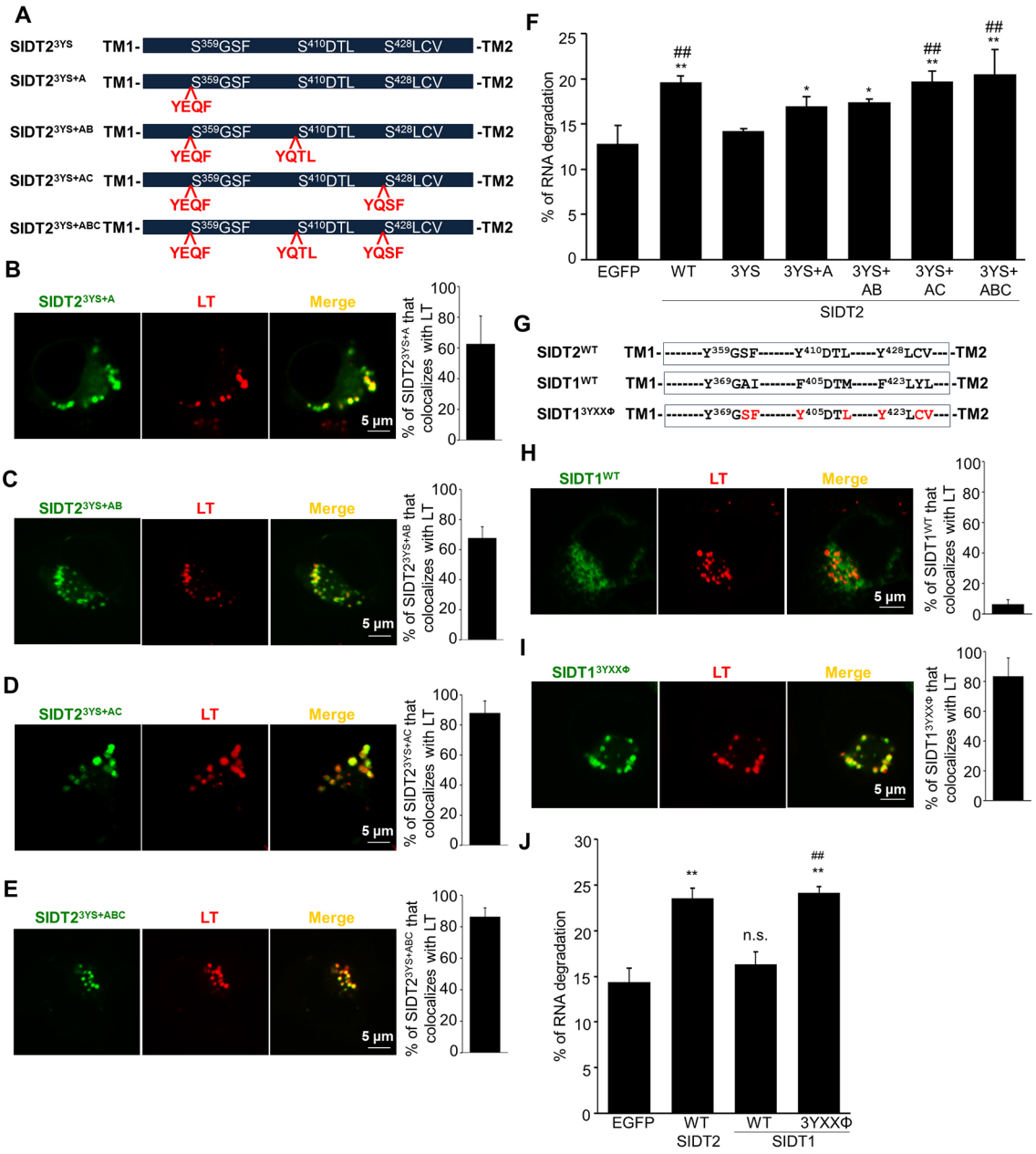

Fig. 6. YGSF, YDTL, and YLCV are functional YxxΦ motifs. (A) Schematic of SIDT2^{3YS} and its mutants. (B–E,H,I) SIDT2-EGFP mutants, SIDT1-EGFP or SIDT1^{3YxxΦ}-EGFP were expressed in Neuro2a cells, and then lysosomes were stained with LT. Image acquisition was performed using a confocal laser-scanning microscope (n=6–8). (G) Schematic of SIDT2^{WT}, SIDT1^{WT} and SIDT1^{3YxxΦ}. The replaced amino acids in SIDT1^{3YxxΦ} are shown in red. (F,J) Neuro2a cells were transfected with expression vectors, then cells were exposed to 0.012 pM [^{3}H]uridine for 24 h to label intracellular RNA. Next, cells were rinsed and grown in culture medium containing 5 mM unlabeled uridine. After 0 and 24 h, the cells were harvested and acid-insoluble radioactivity was measured and expressed as a percentage of degraded RNA. (F) *P<0.05, **P<0.01 vs EGFP; $^{\#\#}P$<0.01 vs 3YS; n=3 (Tukey-Kramer test). (J) **P<0.01 vs EGFP; n.s., not significant vs EGFP; $^{\#\#}P$<0.01 vs WT SIDT1; n=3 (Tukey-Kramer test). Data are mean±s.d. Scale bars: 5 µm.

(Fig. 2C). The Y^{359}GSF motif is located the farthest from the transmembrane domain, and our results showed that disruption of this motif decreased the colocalization rate of SIDT2 with LT the least (Fig. 2E,I). The Y^{410}DTL motif contains an aspartate residue and is the second most distant from the transmembrane domain, while the Y^{428}LCV motif is the closest (Fig. 2B,C). There was no significant difference between the colocalization rates of SIDT2^{Y410S} and SIDT2^{Y428S} (Fig. 2I). This could be because the Y^{410}DTL motif contains an acidic (aspartate) residue that may increase the lysosomal targeting efficiency. Disruption of all three YxxΦ motifs almost completely abolished the localization of SIDT2 to the lysosomal membrane (Fig. 3H). These results showed that the Y^{359}GSF, Y^{410}DTL and Y^{428}LCV motifs are required for the lysosomal localization of SIDT2. Therefore, our study suggests, for the first time, that multiple YxxΦ motifs distant from the transmembrane domain, which are not located at the carboxyl terminus of the protein, can function together to mediate lysosomal targeting. SIDT2 contains a Yxx sequence of amino acids at its carboxyl terminus, 11 residues from the ninth transmembrane domain (Fig. 2B). We demonstrated that this sequence is not part of the signal responsible for the lysosomal localization of SIDT2. Our data suggest that incomplete YxxΦ motifs cannot exert lysosomal

Journal of Cell Science (2017) 130, 2843-2853 doi:10.1242/jcs.202481

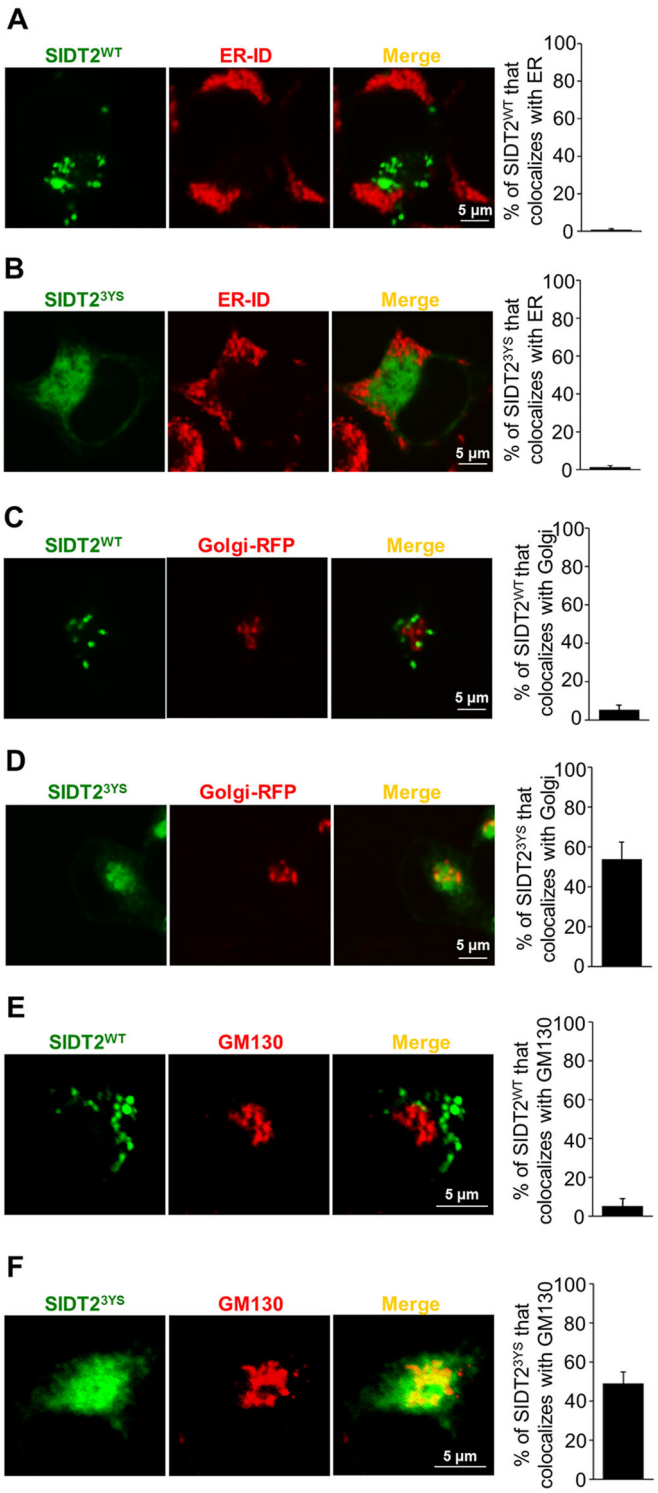

Fig. 7. SIDT2^{3YS} accumulates in the Golgi complex. (A,B) WT or 3YS SIDT2-EGFP was expressed in Neuro2a cells and the ER was stained using an ER-ID Red assay kit. Image acquisition was performed with a confocal laser-scanning microscope and colocalization rates were quantified using ImageJ (n=5). (C,D) WT or 3YS SIDT2-EGFP was expressed in Neuro2a cells and the Golgi complex was stained using CellLight Golgi-RFP BacMam 2.0. Image acquisition was performed using a confocal laser-scanning microscope and colocalization rates were quantified using ImageJ (n=8–9). (E,F) After WT or 3YS SIDT2-EGFP was expressed in Neuro2a cells, the cells were fixed and immunostained using anti-GM130 antibodies. Image acquisition was performed with a confocal laser-scanning microscope and colocalization rates were quantified using ImageJ (n=4–5). Data are mean±s.d. Scale bars: 5 µm.

localization of proteins even though the motifs are located at the carboxyl terminus, close to the transmembrane domain.

Lysosomal membrane proteins are transported to the lysosomes through a direct and/or an indirect pathway. In the direct pathway, proteins are transported from the trans-Golgi network to endosomes and then to lysosomes, while in the indirect pathway proteins are first transported to the cell membrane, then internalized into endosomes and delivered to lysosomes. AP-1 mediates bidirectional transport between the trans-Golgi network and endosomes, while AP-2 functions exclusively on the cell membrane (Bonifacino and Traub, 2003; Braulke and Bonifacino, 2009; Park and Guo, 2014). CoIP and shotgun proteomic analysis revealed that SIDT2 interacts with AP-1 and AP-2 mainly through the YGSF motif (Fig. 4, Table 1; Table S1). These results suggest that SIDT2 is delivered to the lysosomes through both the direct and indirect pathways, and that the YGSF motif partly mediates the delivery. The idea that SIDT2 is delivered to lysosomes at least through the indirect pathway is consistent with our previous study, in which we observed that a part of SIDT2 localizes to the cell membrane in HeLa cells (Takahashi et al., 2017). However, it remains unclear how YDTL and YLCV motifs participate in SIDT2 targeting to the lysosomal membrane.

A closer look at the amino acid sequence between transmembrane 1 and 2 of various SIDT2 homologs revealed that the YxxΦ motifs that mediate the targeting of SIDT2 to the lysosomal membrane are conserved among various species (Fig. 2A). *Xenopus tropicalis* and *Danio rerio* had only two conserved YxxΦ motifs out of the three, suggesting that two motifs may be sufficient for lysosomal localization of SIDT2 in some organisms. SIDT1 has only one YxxΦ motif in its predicted cytosolic regions (Fig. 2A and Fig. 6G) and it scarcely localizes to lysosomes (Fig. 6H). However, overexpression of SIDT1 had a tendency to increase the levels of degraded RNA at the cellular level (Fig. 6J). This result suggests that SIDT1 may be targeted to the lysosomal membrane under a particular set of conditions. Addition of the three YxxΦ motifs that mediate lysosomal localization of SIDT2 to SIDT1 successfully redirected SIDT1 to the lysosomal membrane, indicating that the three YxxΦ motifs are functional and can confer lysosomal localization to a nonlysosomal transmembrane protein. SIDT2 was first identified as an ortholog of the *C. elegans* SID-1 protein together with SIDT1; however, the *C. elegans* CUP-1 protein (also named tag-130) exhibits higher sequence similarity with SIDT2 than SID-1 between transmembrane domains 1 and 2 (Fig. 2A). This observation is consistent with other studies (Pei et al., 2011), and suggests that CUP-1 is an ortholog of SIDT2.

We report here that SIDT2 overexpression markedly increases degradation of RNA at the cellular level. Abnormal expression and accumulation of noncoding RNA repeats in cells are associated with the etiology of various human diseases, such as amyotrophic lateral sclerosis, fragile X syndrome, spinocerebellar ataxia and myotonic dystrophy. It is believed that toxic RNA forms RNA foci in the nucleus and in the cytoplasm, alters the functions of RNA-binding proteins, and exhibits cytotoxicity (Sicot and Gomes-Pereira, 2013). Expanded RNA GGGGCC repeats have been linked to the pathology of amyotrophic lateral sclerosis associated with frontotemporal dementia (DeJesus-Hernandez et al., 2011; Renton et al., 2011). We have reported that GGGGCC repeats can be degraded by RNautophagy *in vitro*, suggesting that RNautophagy may be involved in the degradation of RNA containing GGGGCC repeats in the case of this disease (Hase et al., 2015). Given that SIDT2 overexpression markedly increased RNA degradation at the cellular level, upregulation of SIDT2 activity could be a potential target for developing novel therapies for accumulating toxic RNA-related diseases.

Journal of Cell Science

Journal of Cell Science (2017) 130, 2843-2853 doi:10.1242/jcs.202481

MATERIALS AND METHODS

Chemicals and reagents

Dulbecco's modified Eagle's medium (DMEM) was purchased from Life Technologies. Fetal bovine serum (FBS), Tween 20, sucrose, 3-(N-morpholino)propanesulfonic acid (MOPS), ATP, dimethyl sulphoxide, tris (hydroxymethyl)aminomethane (Tris), Anti-FLAG M2 Affinity Agarose Gel, and monoclonal mouse anti-ACTB/β-actin antibody (AC-15) were purchased from Sigma-Aldrich. Lipofectamine LTX Reagent with PLUS Reagent, LT and TRIzol Reagent were obtained from Life Technologies, and the ER-ID Red Assay Kit was purchased from Enzo Life Sciences. pEGFP-N1 vector was purchased from Clontech Laboratories. Uridine, ethidium bromide, BafA1, monoclonal mouse anti-DYKDDDDK (FLAG) antibody (018-22783), and trichloroacetic acid (TCA) were purchased from Wako Pure Chemical Industries. Ethylenediaminetetraacetic acid (EDTA) and 4-(2-hydroxyethyl)-1-piperazineethanesulfonic acid (HEPES) were supplied by Dojindo Molecular Technologies. Bovine serum albumin (BSA) was obtained from Iwai Chemicals, and polyethyleneimine (PEI) from Polysciences. Monoclonal mouse anti-GM130 antibody (610823) and monoclonal mouse anti-γ-adaptin antibody (610386) were purchased from BD Transduction Laboratories. ProLong Gold antifade reagent with DAPI was purchased from Life Technologies. Alexa Fluor 594-conjugated anti-mouse IgG (ab150108), polyclonal rabbit anti-AP3M1 antibody (ab113104) and polyclonal rabbit anti-AP4M1 antibody (ab96306) were supplied by Abcam. PCI-neo mammalian expression vector was purchased from Promega, and the QuikChange Site-Directed Mutagenesis Kit was obtained from Stratagene Cloning Systems. Lysosome Enrichment Kit for Tissues and Cultured Cells, SuperSignal West Dura Extended Duration Substrate, horseradish peroxidase (HRP)-conjugated anti-rabbit IgG (31460), HRP-conjugated anti-mouse IgG (31430), phosphate-buffered saline (PBS) and CellLight Golgi-RFP BacMam 2.0 Reagent were purchased from Thermo Fisher Scientific. Sodium dodecyl sulfate and phosphatase inhibitor cocktail were purchased from Nacalai Tesque, and cOmplete EDTA-free Protease Inhibitor Cocktail from Roche Diagnostics. The Pierce BCA Protein Assay Kit was purchased from Thermo Fisher Scientific. Polyclonal rabbit anti-SIDT2 antibody (PAB27211) was purchased from Abnova, and [^{3}H]uridine was purchased from PerkinElmer. Monoclonal mouse anti-α-adaptin antibody (sc-17771) was supplied by Santa Cruz Biotechnology. The rabbit polyclonal anti-SIDT2 antibody was raised in a rabbit against synthetic peptides (C+DLDTVQRDKIYVF) containing an amino acid sequence corresponding to the C-terminal of SIDT2.

Cell culture

Murine neuroblastoma Neuro2a cells (Aizawa et al., 2016) were grown in DMEM supplemented with 10% FBS at 37°C under humidified 5% CO_2 atmosphere. Cell passage was performed every time the cells were 80–100% confluent. Cells cultivated up to 2 months were generally used in experiments. We used Neuro2a cells because we have previously shown that the localization of SIDT2-EGFP to lysosomes and lysosomal compartments can be clearly observed in these cells (Aizawa et al., 2016).

Live cell imaging

Neuro2a cells were seeded at 3×10^5 cells/dish in 35 mm glass-bottom μ-dishes (ibidi GmbH) and incubated for 24 h, followed by transient transfection with each of the pEGFP-N1 vectors (0.5 μg/dish) using Lipofectamine LTX Reagent with PLUS Reagent, according to the manufacturer's instructions. At 24 hours post-transfection, cells were incubated with 100 nM LT diluted in growth medium to label lysosomes. We used an ER-ID Red assay kit to label the ER. At 24 hours post-transfection, cells were incubated for 30 min with the detection reagent diluted (1:10,000) in assay buffer containing 5% FBS. Then, cells were rinsed with PBS and returned to the growth medium. CellLight Golgi-RFP BacMam 2.0 Reagent was used to stain the Golgi complex. Neuro2a cells were seeded at 1×10^5 cells/well in four-well glass-bottom μ-slides (ibidi GmbH) and incubated for 18 h, followed by addition of the CellLight Reagent (50 μl/well) and transient transfection with each of the pEGFP-N1 vectors (0.1 μg/well) concomitantly. After 24 h, cells were imaged. Image acquisition was performed using a FLUOVIEW FV10i confocal microscope (Olympus). Quantification and calculation of colocalization rates were performed with ImageJ software via the JACoP plugin, as previously described (Bolte and Cordelières, 2006; Cordelières, 2008).

Immunofluorescent staining

Neuro2a cells were seeded (1×10^5 cells/well) on two-well chamber slides (Nalge Nunc International) and incubated for 24 h, and then transient transfection with each of the pEGFP-N1 vectors (0.2 μg/well) was performed using Lipofectamine LTX Reagent with PLUS Reagent, according to the manufacturer's instructions. At 24 hours post-transfection, the medium was removed and cells were fixed for 20 min with 3.7% formaldehyde at room temperature, and then permeabilized for 5 min with 0.1% Tween 20. After blocking for 1 h with 3% BSA at room temperature, the cells were incubated with anti-GM130 antibodies (1:250) in 3% BSA overnight at 4°C, and then with Alexa Fluor 594-conjugated secondary antibodies (1:500) for 1 h at room temperature. All reagents were prepared in PBS unless indicated otherwise. Cells were rinsed with PBS before each step. Slides were mounted with ProLong Gold antifade reagent with DAPI overnight, and image acquisition was performed using a confocal laser microscope (FV1000DIX81, Olympus). Quantification and calculation of colocalization rates were performed with ImageJ software via the JACoP plugin.

Plasmid generation

The pCI-neo-mSIDT2, pEGFP-mSIDT2, pCI-neo-mSIDT1 and pEGFP-mSIDT1 plasmids were prepared as described previously (Aizawa et al., 2016). Plasmids for expression of SIDT2 and SIDT1 mutants were generated using the QuikChange Site-Directed Mutagenesis Kit according to the manufacturer's instructions. To generate pCI-neo-mSIDT2-FLAG for the expression of FLAG-tagged SIDT2 with a FLAG tag between Gly-24 and Pro-25, a DNA sequence encoding FLAG was inserted using the QuikChange Mutagenesis Kit according to the manufacturer's instructions. All resulting constructs were confirmed by sequencing.

Total RNA extraction and RNA uptake by isolated lysosomes

Total RNA was extracted from mouse brains using TRIzol Reagent according to the manufacturer's instructions. The total RNA concentration was measured with a NanoDrop 1000 Spectrophotometer (Thermo Fisher Scientific). All animal experiments were approved by the animal committee of the National Center of Neurology and Psychiatry.

Lysosomes were isolated from 0.7–1×10^8 Neuro2a cells by density gradient centrifugation using a Lysosome Enrichment Kit for Tissues and Cultured Cells, rinsed, and resuspended in 0.3 M sucrose. Isolated lysosomes (20–30 μg protein) were incubated with 5 μg total RNA at 37°C for 3 min in 30 μl buffer (pH 7) containing 10 mM MOPS, 0.3 M sucrose and 10 mM ATP. The mixture was then quenched and lysosomes were removed by centrifugation. The level of RNA remaining in the supernatant was examined by agarose gel electrophoresis with ethidium bromide staining and UV illumination using a FluorChem 8000 imaging system (AlphaInnotech). Signal intensity was quantified with ImageJ software.

Immunoprecipitation and shotgun proteomic analysis

Neuro2a cells were seeded at 3×10^6 cells/dish on 10 cm plastic dishes and grown for 24 h, and then transfected with 5 μg of vectors expressing WT or FLAG-tagged SIDT2 using 1 mg/ml PEI (20 μl/dish). At 24 hours post-transfection, cells were harvested and suspended in a lysis buffer containing 50 mM HEPES-NaOH, pH 7.6, 150 mM KCl, 5% glycerol (v/v) and 1% nonaethylene glycol monododecyl ether (v/v), supplemented with protease and phosphatase inhibitors according to the manufacturer's instructions. After incubation at 4°C with rotation for 20 min, cell lysates were centrifugated (15,000×***g***, 15 min) at 4°C, and the supernatant was incubated at 4°C for 1 h with anti-FLAG M2 agarose affinity gel prewashed three times with lysis buffer. Next, the agarose beads were washed three times with the lysis buffer, elution was performed with Laemmli sample buffer (Laemmli, 1970), and immunoblotting was performed (Aizawa et al., 2016). For mass spectrometry (MS) analysis, the agarose beads were additionally washed twice with a wash buffer containing 25 mM Tris-HCl, pH 7.6 and 150 mM NaCl, supplemented with phosphatase inhibitors, then elution was performed using 100 μl of 100 μg/ml FLAG peptide in wash buffer/dish, followed by tryptic digestion.

Shotgun proteomic analyses were performed by a linear ion trap-orbitrap mass spectrometer (LTQ-Orbitrap Velos, Thermo Fisher Scientific) coupled with nanoflow LC system (Dina-2A, KYA Technologies). Peptides were injected into a 75 µm reversed-phase C18 column at a flow rate of 10 µl/min, and eluted with a linear gradient of solvent A (2% acetonitrile and 0.1% formic acid in H_2O) to solvent B (40% acetonitrile and 0.1% formic acid in H_2O) at 300 nl/min. Peptides were sequentially sprayed from a nanoelectrospray ion source (KYA Technologies) and analyzed by collision-induced dissociation. The analyses were operated in data-dependent mode, switching automatically between MS and tandem mass spectrometry (MS/MS) acquisition. For collision-induced dissociation analyses, full-scan MS spectra (from 380 to 2000 *m/z*) were acquired in the orbitrap with resolution of 100,000 at 400 *m/z* after ion count accumulation to the target value of 1,000,000. The 20 most intense ions at a threshold above 2000 were fragmented in the linear ion trap with normalized collision energy of 35% for an activation time of 10 ms. The orbitrap analyzer was operated with the 'lock mass' option to perform shotgun detection with high accuracy. Protein identification was conducted by searching MS and MS/MS data against the RefSeq (National Center for Biotechnology Information) mouse protein database (29,579 protein sequences as of 4 February, 2013) by Mascot version 2.5.1 (Matrix Science). Carbamidomethylation of cysteine was set as a fixed modification. Methionine oxidation; protein N-terminal acetylation; pyroglutamination for N-terminal glutamine; phosphorylation of serine, threonine and tyrosine; and glycylglycine-modified lysine were set as variable modifications. A maximum of two missed cleavages was allowed in our database search, while the mass tolerance was set to 3 ppm for peptide masses and 0.8 Da for MS/MS peaks, respectively. In the process of peptide identification, we conducted decoy database searching by Mascot and applied a filter to satisfy a false positive rate <1%.

Western blotting

Cells were washed with PBS and then lysed in lysis buffer (2% sodium dodecyl sulfate, 50 mM Tris buffer, pH 7.8, 150 mM NaCl, 20 mM EDTA) supplemented with protease inhibitors, according to the manufacturer's instructions. Protein concentration was determined using the Pierce BCA Protein Assay Kit according to the manufacturer's instructions. Cell lysates were mixed with Laemmli sample buffer. Equal amounts of protein were loaded and separated by SDS-PAGE, and then transferred onto a PVDF membrane. The membrane was blocked for 30 min with 3% BSA in PBS, and then incubated overnight at 4°C with primary antibodies diluted in PBS containing 3% BSA for detection of SIDT2 (1:1000), γ-adaptin (1:1000), α-adaptin (1:1000), FLAG (1:2000), AP-3 µ1 subunit (1:500), AP-4 µ1 subunit (1:1000) or β-actin (1:5000). After washing, incubation with secondary antibodies was performed for 1–2 h at room temperature. The antibodies were diluted in PBS containing 0.1% (v/v) Tween 20 for detection of SIDT2 (1:5000), γ-adaptin (1:5000), α-adaptin (1:5000), FLAG (1:20,000), AP-3 µ1 subunit (1:5000), AP-4 µ1 subunit (1:5000) or β-actin (1:10,000). Immunoreactive signals were visualized using SuperSignal West Dura Extended Duration Substrate and detected with a FluorChem 8000 imaging system. Signal intensity was quantified using ImageJ.

Measurement of endogenous RNA degradation

RNA degradation was measured as described previously (Aizawa et al., 2016), using a different cell line. Neuro2a cells were seeded at 2×10^5 cells/well in 12-well culture plates and grown for 24 h, and then cotransfected with each vector together with carrier DNA (pCI-neo vector) up to 0.2 µg DNA/well, using 1 mg/ml PEI (0.8 µl/well) dissolved in buffer containing 25 mM HEPES, pH 7 and 150 mM NaCl. Addition of carrier DNA was reported to increase transfection efficiency, especially when the amount of plasmid DNA is low (Pradhan and Gadgil, 2012). At 24 hours post-transfection, 0.3 µCi/ml [^{3}H]uridine was added for RNA labeling. At 24 hours post-labeling, cells were rinsed and cultured in culture medium containing 5 mM unlabeled uridine. After 0 and 24 h of incubation, cells were trypsinized and TCA-insoluble radioactivity was measured using a Tri-Carb 3100TR Low Activity Liquid Scintillation Analyzer (PerkinElmer). Radioactivity is expressed as a percentage of radioactivity at 0 h.

Statistical analysis

Analysis of variance with the Tukey-Kramer test was used for comparisons of two or more groups.

Acknowledgements

We thank Dr Yosuke Yoneyama for providing us with useful information on antibodies and Yoshiko Hara for technical support.

Competing interests

The authors declare no competing or financial interests.

Author contributions

Conceptualization: V.R.C., T.K.; Methodology: V.R.C., K.H., Y.F., K.W., T.K.; Validation: V.R.C., K.H., Y.F., T.K.; Investigation: V.R.C., K.H., H.K.-H., M.O., Y.F., C.K., M.T., F.H., S.-I.T., T.K.; Writing - original draft: V.R.C.; Writing - review & editing: V.R.C., T.K.; Supervision: T.K.; Project administration: T.K.; Funding acquisition: V.R.C., K.W., T.K.

Funding

This work was supported by the Japan Society for the Promotion of Science (24680038, 26111526, 16H05146 and 16H01211 to T.K.; 25290027 to K.W.; 15J06173 to V.R.C.) and Japan Agency for Medical Research and Development (16ek0109048h to K.W.).

Supplementary information

Supplementary information available online at
http://jcs.biologists.org/lookup/doi/10.1242/jcs.202481.supplemental

References

Aizawa, S., Fujiwara, Y., Contu, V. R., Hase, K., Takahashi, M., Kikuchi, H., Kabuta, C., Wada, K. and Kabuta, T. (2016). Lysosomal putative RNA transporter SIDT2 mediates direct uptake of RNA by lysosomes. *Autophagy* **12**, 565-578.

Aizawa, S., Contu, V. R., Fujiwara, Y., Hase, K., Kikuchi, H., Kabuta, C., Wada, K. and Kabuta, T. (2017). Lysosomal membrane protein SIDT2 mediates the direct uptake of DNA by lysosomes. *Autophagy* **13**, 218-222.

Bolte, S. and Cordelières, F. P. (2006). A guided tour into subcellular colocalization analysis in light microscopy. *J. Microsc.* **224**, 213-232.

Bonifacino, J. S. and Traub, L. M. (2003). Signals for sorting of transmembrane proteins to endosomes and lysosomes. *Annu. Rev. Biochem.* **72**, 395-447.

Braulke, T. and Bonifacino, J. S. (2009). Sorting of lysosomal proteins. *Biochim. Biophys. Acta* **1793**, 605-614.

Chapel, A., Kieffer-Jaquinod, S., Sagné, C., Verdon, Q., Ivaldi, C., Mellal, M., Thirion, J., Jadot, M., Bruley, C., Garin, J. et al. (2013). An extended proteome map of the lysosomal membrane reveals novel potential transporters. *Mol. Cell. Proteomics* **12**, 1572-1588.

Cordelières, F. P. (2008). JACoP v2.0: improving the user experience with co-localization studies. In ImageJ User and Developer Conference, pp. 174-181.

DeJesus-Hernandez, M., Mackenzie, I. R., Boeve, B. F., Boxer, A. L., Baker, M., Rutherford, N. J., Nicholson, A. M., Finch, N. A., Flynn, H., Adamson, J. et al. (2011). Expanded GGGGCC hexanucleotide repeat in noncoding region of C9ORF72 causes chromosome 9p-linked FTD and ALS. *Neuron* **72**, 245-256.

Duxbury, M. S., Ashley, S. W. and Whang, E. E. (2005). RNA interference: a mammalian SID-1 homologue enhances siRNA uptake and gene silencing efficacy in human cells. *Biochem. Biophys. Res. Commun.* **331**, 459-463.

Feinberg, E. H. and Hunter, C. P. (2003). Transport of dsRNA into cells by the transmembrane protein SID-1. *Science* **301**, 1545-1547.

Frankel, L. B., Lubas, M. and Lund, A. H. (2017). Emerging connections between RNA and autophagy. *Autophagy* **13**, 3-23.

Fujiwara, Y., Furuta, A., Kikuchi, H., Aizawa, S., Hatanaka, Y., Konya, C., Uchida, K., Yoshimura, A., Tamai, Y., Wada, K. et al. (2013a). Discovery of a novel type of autophagy targeting RNA. *Autophagy* **9**, 403-409.

Fujiwara, Y., Hase, K., Wada, K. and Kabuta, T. (2015). An RNautophagy/DNautophagy receptor, LAMP2C, possesses an arginine-rich motif that mediates RNA/DNA-binding. *Biochem. Biophys. Res. Commun.* **460**, 281-286.

Fujiwara, Y., Kikuchi, H., Aizawa, S. Furuta, A. Hatanaka, Y. Konya, C. Uchida, K. Wada, K. and Kabuta, T. (2013b). Direct uptake and degradation of DNA by lysosomes. *Autophagy* **9**, 1167-1171.

Fujiwara, Y., Wada, K. and Kabuta, T. (2017). Lysosomal degradation of intracellular nucleic acids-multiple autophagic pathways. *J. Biochem.* **161**, 145-154.

Hase, K., Fujiwara, Y., Kikuchi, H., Aizawa, S., Hakuno, F., Takahashi, S.-I., Wada, K. and Kabuta, T. (2015). RNautophagy/DNautophagy possesses selectivity for RNA/DNA substrates. *Nucleic Acids Res.* **43**, 6439-6449.

Haud, N., Kara, F., Diekmann, S., Henneke, M., Willer, J. R., Hillwig, M. S., Gregg, R. G., Macintosh, G. C., Gärtner, J., Alia, A. et al. (2011). rnaset2 mutant zebrafish model familial cystic leukoencephalopathy and reveal a role for RNase T2 in degrading ribosomal RNA. *Proc. Natl. Acad. Sci. USA* **108**, 1099-1103.

Henneke, M., Diekmann, S., Ohlenbusch, A., Kaiser, J., Engelbrecht, V., Kohlschütter, A., Krätzner, R., Madruga-Garrido, M., Mayer, M., Opitz, L. et al. (2009). RNASET2-deficient cystic leukoencephalopathy resembles congenital cytomegalovirus brain infection. *Nat. Genet.* **41**, 773-775.

Houseley, J. and Tollervey, D. (2009). The many pathways of RNA degradation. *Cell* **136**, 763-776.

Jackowiak, P., Nowacka, M., Strozycki, P. M. and Figlerowicz, M. (2011). RNA degradome - its biogenesis and functions. *Nucleic Acids Res.* **39**, 7361-7370.

Jialin, G., Xuefan, G. and Huiwen, Z. (2010). SID1 transmembrane family, member 2 (Sidt2): a novel lysosomal membrane protein. *Biochem. Biophys. Res. Commun.* **402**, 588-594.

Laemmli, U. K. (1970). Cleavage of structural proteins during the assembly of the head of bacteriophage T4. *Nature* **227**, 680-685.

Park, S. Y. and Guo, X. (2014). Adaptor protein complexes and intracellular transport. *Biosci. Rep.* **34**, e00123.

Pei, J., Millay, D. P., Olson, E. N. and Grishin, N. V. (2011). CREST - a large and diverse superfamily of putative transmembrane hydrolases. *Biol. Direct* **6**, 37.

Pradhan, K. and Gadgil, M. (2012). Effect of addition of 'carrier' DNA during transient protein expression in suspension CHO culture. *Cytotechnology* **64**, 613-622.

Renton, A. E., Majounie, E., Waite, A., Simón-Sánchez, J., Rollinson, S., Gibbs, J. R., Schymick, J. C., Laaksovirta, H., van Swieten, J. C., Myllykangas, L. et al. (2011). A hexanucleotide repeat expansion in C9ORF72 is the cause of chromosome 9p21-linked ALS-FTD. *Neuron* **72**, 257-268.

Schröder, B., Wrocklage, C., Pan, C., Jäger, R., Kösters, B., Schäfer, H., Elsässer, H.-P., Mann, M. and Hasilik, A. (2007). Integral and associated lysosomal membrane proteins. *Traffic* **8**, 1676-1686.

Sicot, G. and Gomes-Pereira, M. (2013). RNA toxicity in human disease and animal models: from the uncovering of a new mechanism to the development of promising therapies. *Biochim. Biophys. Acta* **1832**, 1390-1409.

Takahashi, M., Contu, V. R., Kabuta, C., Hase, K., Fujiwara, Y., Wada, K. and Kabuta, T. (2017). SIDT2 mediates gymnosis, the uptake of naked single-stranded oligonucleotides into living cells. *RNA Biol.* doi: 10.1080/15476286.2017.1302641 [Epub ahead of print].

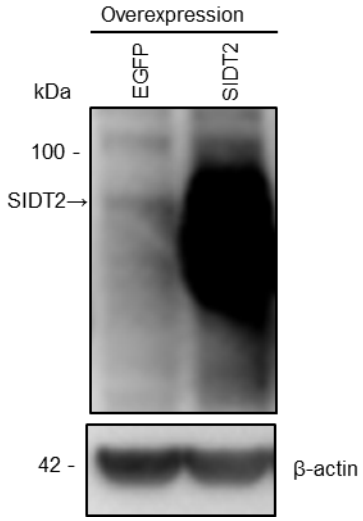

Figure S1. Western blot analysis of SIDT2.

Neuro2a cells were transfected with EGFP- or SIDT2^{WT}-expressing vectors and after 48 h, cells were harvested and cell lysates were immunoblotted using a rabbit polyclonal anti-SIDT2 antibody and a mouse monoclonal anti-β-actin antibody.

The rabbit polyclonal anti-SIDT2 antibody was raised in a rabbit against synthetic peptides (C+DLDTVQRDKIYVF) containing an amino acid sequence corresponding to the C-terminal of SIDT2.

Table S1.
Peptides corresponding to AP subunits identified by shotgun proteomic analysis

Accession Number	Protein Name	Peptide Sequence	Ion Score
21313640	AP-2 complex subunit beta isoform b	LTNGIWILAELR	93
		LASQANIAQVLAELK	87
		KPSETQELVQQVLSLATQDSDNPDLR	78
		LQNNNVYTIAK	59
		DLIADSNPMVVANAVAALSEISESHPNSNLLDLNPQNINK	58
		LVYLYLMNYAK	57
		LSHANSAVVLSAVK	50
		LLTALNECTEWGQIFILDCLSNYNPK	46
		ITEYLCEPLRK	33
		KGEIFELK	33
		NINLIVQK	32
		GLEISGTFTHR	27
88853578	AP-1 complex subunit beta-1 isoform 2	LASQANIAQVLAELK	87
		LVYLYLMNYAK	57
		LSHANSAVVLSAVK	50
		LQSSNIFTVAK	44
		LQSSNIFTVAK	41
		NNIDVFYFSTLYPLHVLFVEDGK	37
		ITEYLCEPLRK	33
		KGEIFELK	33
		NINLIVQK	32
		NNIDVFYFSTLYPLHVLFVEDGK	32
116256510	AP-2 complex subunit alpha-1 isoform b	LLQCYPPPEDAAVK	54
		NPTFMCLALHCIANVGSR	49
		LLQCYPPPEDAAVK	47
		LLQCYPPPEDAAVK	45
		TSVQFQNFLPTVVHPGDLQTQLAVQTK	45
		LLQCYPPPEDAAVK	40
		ANHPMDAEVTK	35
		DFLTPPLLSVR	33
		ILVAGDSMDSVK	28

163644277	AP-2 complex subunit alpha-2	IIGFGSALLEEVDPNPANFVGAGIIHTK	113
		YGGTFQNVSVK	66
		NAVLFEAISLIIHHDSEPNLLVR	39
		TTQIGCLLR	33
6671557	AP-1 complex subunit mu-1	LETGAPRPPATVTNAVSWR	47
		LETGAPRPPATVTNAVSWR	46
		STANNVEIHIPVPNDADSPK	32
		STANNVEIHIPVPNDADSPK	29
		HNNLYLVATSK	28
6753074	AP-2 complex subunit mu	ASENAIVWK	44
		SISFIPPDGEFELMR	36
		LNYSDHDVIK	34
		QSIAIDDCTFHQCVR	29

Untagged SIDT2^{WT} (control) or FLAG-tagged SIDT2^{WT} were expressed in neuro2a cells, the cell lysates were subjected to IP using an anti-FLAG antibody, then shotgun proteomic analysis of the IP products was performed. Peptides corresponding to AP-1 or AP-2 subunits were not detected in the IP-product from the control sample.